Single-Particle Neutron Bound States in Iron Isotopes and in Cobalt Studied with (p,d) Reactions

C. D. GOODMAN, J. B. BALL, AND C. B. FULMER
Oak Ridge National Laboratory, Oak Ridge, Tennessee*
(Received March 12, 1962)

The energy spectra of deuterons from (p,d) reactions in Fe^{54}, Fe^{56}, Fe^{57}, Fe^{58}, and Co^{59} targets were experimentally measured and angular distributions obtained for the more prominent deuteron groups. Reduced widths for exciting various final states differ widely from state to state. The deuteron groups corresponding to the strongly excited states have angular distributions which fit distorted-wave calculations for angular momentum changes of one and of three units. The energies of these groups progress systematically through the sequence of isotopes, and an attempt is made to interpret the groups in terms of single-particle neutron bound states. Definite evidence for strong residual interactions is observed. The locations and number of states suggest the applicability of the Nilsson model with the assumption that Fe^{54} and Co^{59} are spherical and that Fe^{56}, Fe^{57}, and Fe^{58} are deformed in a prolate configuration.

INTRODUCTION

IT has been shown that (p,d)[1] and (p,t)[2] reactions selectively excite certain of the many possible final states of the reactions. In references 1 and 2 the states are interpreted in terms of a direct pickup model of the reaction and a single particle shell model of the nucleus. The strongly excited states are assumed to be those which have the same shell configuration as the target with the picked-up neutron or neutrons missing.

We feel that comparison of the deuteron spectra from neighboring isotopes is essential in the interpretation of the levels. Iron was chosen for this study because of the availability of isotopically enriched metallic foils of each of the four stable isotopes of iron.

The present work is an attempt to use the selectivity of the (p,d) reactions as an aid in interpreting the level schemes of the iron isotopes.

METHOD

The experimental method and the apparatus are described in references 1 and 2. Briefly, the 22.3-MeV external proton beam of the ORNL 86-in. cyclotron strikes a target in a scattering chamber. The emergent charged particles are detected with a dE/dx—E counter system. A pulse multiplier is used to permit recording of the spectra of protons and deuterons in separate halves of a 400-channel analyzer. Thus, 200-channel spectra for each particle type are obtained simultaneously.

TABLE I. Thicknesses and isotopic abundances of targets.

Target	Thickness (mg/cm²)	Composition (%) Fe^{54}	Fe^{56}	Fe^{57}	Fe^{58}	Co^{59}
Natural Fe	7.50	5.9	91.6	2.2	0.33	...
Fe^{54}	5.4	94.7	5.1	0.2	0.0	...
Fe^{56}	1.4	<0.1	99.9	<0.1	0.0	...
Fe^{57}	3.1	0.3	23.0	76.7	0.1	...
Fe^{58}	1.3	0.5	19.7	2.5	77.2	...
Co^{59}	3.4	...	...	...	...	100

For the recent runs, a surface-barrier counter made on a 0.004-in. wafer of silicon was used instead of the proportional counter for the dE/dx measurement. This counter has better gain stability than the proportional counter, and the small physical thickness of the mounted solid state counter (less than 1/2 in.) simplifies the problem of avoiding particle loss due to misalignment of the front and back windows of the long (4 in.) proportional counter or due to multiple scattering in the front window and counter gas.

The beam was monitored with a Faraday cup and current integrator. A scintillation counter, set to count elastically scattered protons from the target at a fixed angle of 45°, was used as an additional check on the normalization of the points in the angular distributions and was used to normalize the data taken at angles smaller than 15°, for which the Faraday cup had to be removed.

The targets were self-supporting metallic foils with isotopic enrichments shown in Table I. The Fe^{54}, Fe^{57}, natural Fe, and Co^{59} targets were rolled foils, and the Fe^{56} and Fe^{58} targets were electroplated foils.[3]

Counting loss due to dead time of the multichannel analyzer was evaluated in the manner described in reference 2. The beam current was limited to keep the counting loss below 5%, except at the extreme forward angles where some runs were made with up to 10% counting loss. This restriction set the time required to obtain a spectrum with statistics as shown in the figures at three to four hours.

The raw data from the analyzer were automatically punched out on an IBM 024 card punch. Transformation of the raw data to corrected energy spectra was

* Operated for the U. S. Atomic Energy Commission by Union Carbide Corporation.

[1] C. D. Goodman and J. B. Ball, Phys. Rev. **118**, 1062 (1960).

[2] J. B. Ball and C. D. Goodman, Phys. Rev. **120**, 488 (1960).

[3] The Fe^{54} and Fe^{57} targets were rolled by Frank Karasek of Argonne National Laboratory. The Fe^{56} and Fe^{58} targets were prepared by Robert Seegmiller of Los Alamos Scientific Laboratory, and the natural iron and cobalt foils were purchased from the A. D. MacKay Company, New York, N. Y. The isotopically enriched materials were obtained from the Isotopes Division of Oak Ridge National Laboratory.

accomplished with the aid of the CONDAC program[4] and an IBM 7090 computer. The output from the computer, in the form of punched cards, was then plotted automatically using a Moseley plotter attached to the 024 card punch reading station.

The energy scale in the processed data depends on the incident energy, which is subject to drifts, and on the effective absorber between the target and the E counter, which is not known precisely because of the impossibility of weighing the dE/dx counter directly. In the spectra shown in the figures, the beam energy was assumed to be 22.3 MeV and the effective absorber was determined by setting $Q=0$ for the elastically scattered protons and $Q=-9.0$ MeV for the ground-state deuteron group from $Fe^{56}(p,d)Fe^{55}$. When the 0.004-in. solid state dE/dx counter is used, the effective absorber thickness is 33 mg/cm^2 (aluminum equivalent) plus one-half the target thickness.

The measured Q values are not more accurate than ± 0.1 MeV, and at very negative Q values, where the determination is more sensitive to uncertainties in the beam energy and absorber, the errors may be larger. An error of as much as ± 0.3 MeV near $Q=-12$ MeV cannot be ruled out.

For the determination of absolute cross sections the target thicknesses were determined by weighing and measuring the areas of the rolled foils. The electroplated foils (Fe^{56} and Fe^{58}) could not be weighed because they could not be removed nondestructively from their frames. The thicknesses of these foils were determined by comparing the elastic scattering intensities at 18° laboratory angle to those from the weighed foils. The thicknesses determined in this manner for the foils which could also be weighed were in agreement with the weighed values.

The principal sources of error in the absolute cross sections are uncertainties in (1) the target thickness, (2) the total integrated beam current, (3) the solid angle subtended by the counter, (4) the total number of counts assigned to an imperfectly resolved peak, and (5) the number of counts lost due to imperfect separation of particle types. Items 4 and 5 contribute most of the uncertainty in the cross sections. We estimate that the over-all uncertainty is of the order of 10% of the total count, depending on the individual case. The target thicknesses are known to about 5%, and the integrated beam current and the solid angle are each known to about 1%.

RESULTS

Figures 1–6 show representative deuteron spectra from (p,d) reactions on the iron isotopes and cobalt. Many of the Fe^{56} data points were obtained with a natural iron target. Spectra are shown for enriched and natural targets. The only significant difference between the two spectra is the absence of the $Fe^{54}(p,d)$ ground state group ($Q=-11.2$ MeV) in the spectrum from the enriched target. The error flags in the spectra indicate statistics only.

Figure 7 shows the differential cross section for $Fe^{54}(p,d)Fe^{53}$ to the ground state of Fe^{53}. The data points are obtained by summing the counts in the peaks in the appropriate spectra. Some degree of arbitrary judgment is unavoidable in this summation; this represents a major part of the uncertainty in the cross section. As noted above, the over-all uncertainty is estimated to be about 10%. The error flags represent the statistical uncertainty only. The solid curve is the theoretical cross section described below. Figures 8 and 9 show observed and calculated differential cross sections for two peaks in the $Fe^{56}(p,d)Fe^{55}$ spectrum.

The theoretical cross sections shown in Figs. 7–9 were calculated by Bassel, Drisko, and Satchler with a computer code called "Sally."[5] The calculation uses distorted wave direct interaction theory in which optical model potentials are used for the incoming and outgoing channel. The choice of potentials is restricted

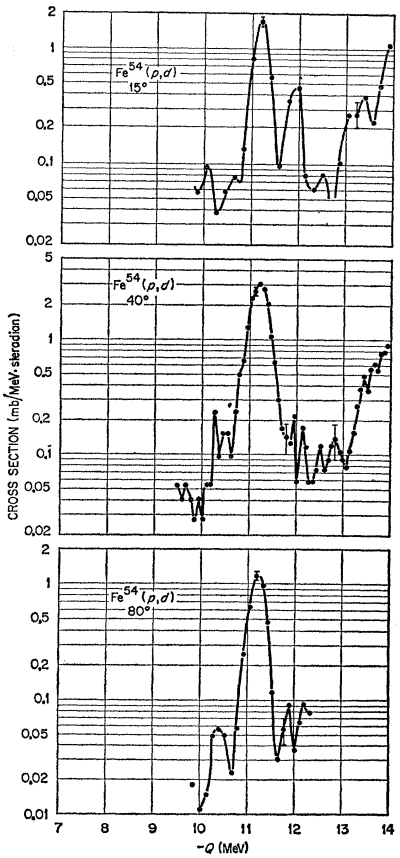

FIG. 1. Spectra for $Fe^{54}(p,d)$ at 15, 40, and 80 degrees.

[4] C. D. Goodman and B. D. Williams, Oak Ridge National Laboratory Report ORNL-2925, 1960 (unpublished).

[5] R. H. Bassel, R. M. Drisko, and G. R. Satchler, Oak Ridge National Laboratory Report ORNL-3240, 1962 (unpublished).

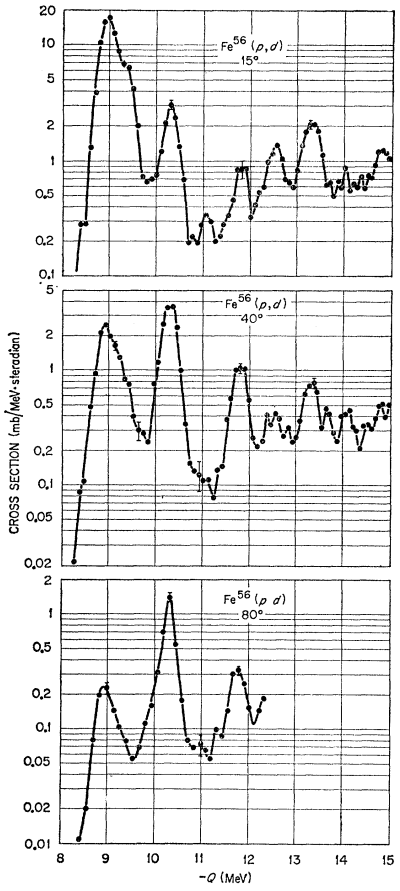

FIG. 2. Spectra for $Fe^{56}(p,d)$ at 15, 40, and 80 degrees.

to those which fit the appropriate proton elastic scattering data. The deuteron-nucleus potential does not result in a good fit to the deuteron elastic scattering data, and it is hoped that a better potential can be found.[6] The calculated cross section is that for the pickup of a single neutron from the $1f_{7/2}$ or the $2p_{3/2}$ shell model state.

The distorted wave calculations have the advantage over Butler-Born approximation plane-wave calculations that the calculated shape of the angular distribution agrees with the observed shape over a large angular range. The absolute cross sections are closer to the experimentally observed values than are the plane wave values and the relative values of cross sections for different angular momentum changes are believed to be predicted correctly.

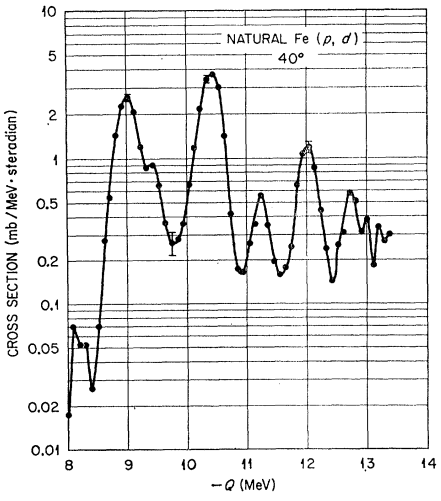

FIG. 3. (p,d) spectrum for natural iron at 40 degrees.

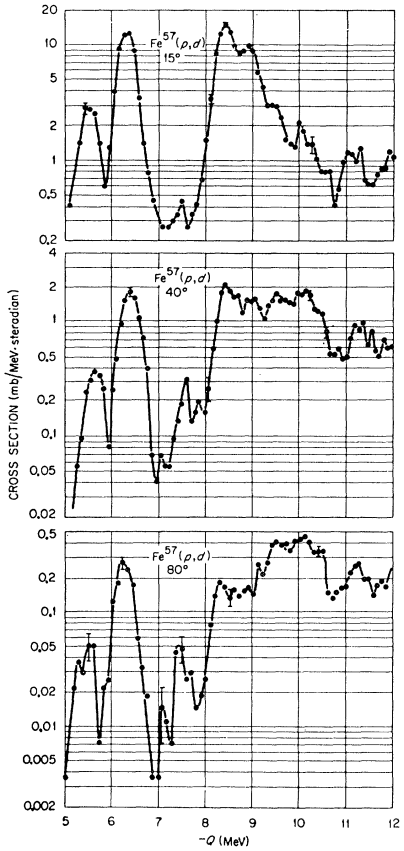

FIG. 4. Spectra for $Fe^{57}(p,d)$ at 15, 40, and 80 degrees.

Table II lists the ratios S of measured cross section to calculated cross section for the various peaks in the spectra. These ratios are determined by requiring a good match between the calculated and observed cross sections to about 60° and ignoring the data beyond

[6] A complete description of the potentials used in the calculation can be found in reference 5. The proton-nucleus potential is a Saxon-Woods well with a real depth of 48 MeV and an imaginary depth of 13 MeV. The Coulomb and optical potential radii are both $1.26A^{\frac{1}{3}}$ F. The diffuseness parameter is 0.51 F. The deuteron-nucleus potential is a Saxon-Woods real well with a surface Gaussian imaginary well. The well depth is 85 MeV real and 20 MeV imaginary. The real well radius is $1.5A^{\frac{1}{3}}$ F. The Coulomb radius is $1.1A^{\frac{1}{3}}$ F. The diffuseness parameter is 0.61 F. The Gaussian radius is $1.5A^{\frac{1}{3}}$ F and the Gaussian width is 1.2 F.

that angle. This is probably a reasonable procedure since the large-angle points are expected to have less theoretical validity than the small-angle points. The factors S have the same interpretation as the spectroscopic factors of Macfarlane and French.[7]

Spectroscopic factors greater than unity are expected for the pickup from a shell occupied by several equivalent particles. In the simple case of equivalent particles occupying a degenerate shell-model state, the spectroscopic factor represents the number of particles occupying the state.

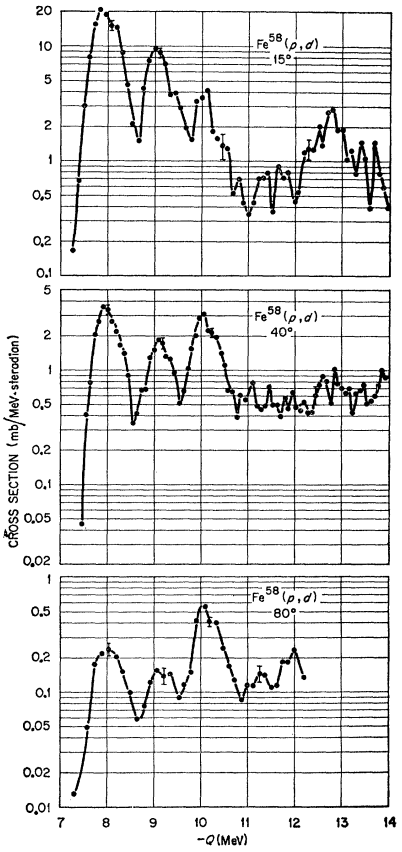

FIG. 5. Spectra for $Fe^{58}(p,d)$ at 15, 40, and 80 degrees.

DISCUSSION

The single-particle shell model provides a convenient framework in which to understand the selectivity of the (p,d) reaction. One may picture the neutrons in the target nucleus in single-particle bound states. The reaction removes one of the neutrons leaving a single hole in the original neutron configuration, and, to a first approximation, only those final states which can be described as single-neutron holes in the target configuration are excited.

This oversimplified model accounts for several of the gross features of the (p,d) spectra, namely, the appearance of only $l=1$ and $l=3$ angular distributions in the iron region, where the shell model predicts p and f bound states, and the fact that the (p,d) spectra from targets of a given neutron number generally resemble those from targets with lower neutron number with the addition of new peaks.

The simplest model would regard the 28 neutrons in Fe^{54} as a closed shell core and would treat Fe^{56}, Fe^{57}, and Fe^{58} as 2, 3, and 4 neutrons in the $p_{3/2}$ shell. It is

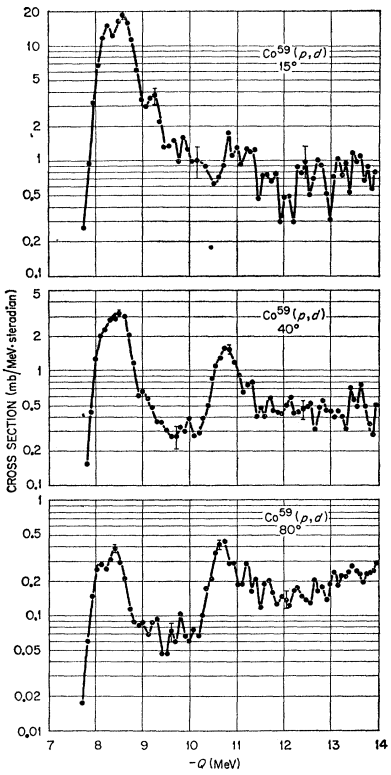

FIG. 6. Spectra for $Co^{59}(p,d)$ at 15, 40, and 80 degrees.

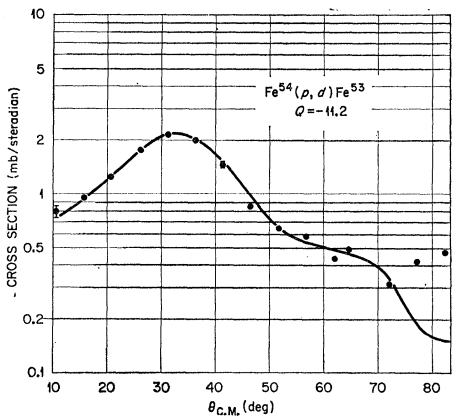

FIG. 7. Angular distribution of the deuteron group leading to the ground state in the reaction $Fe^{54}(p,d)Fe^{53}$. The solid curve is a distorted-wave Born-approximation calculation.

[7] M. H. Macfarlane and J. B. French, Revs. Modern Phys. **32**, 565 (1960).

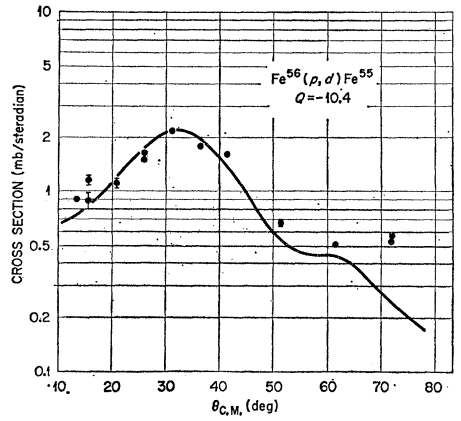

FIG. 8. Angular distribution of the deuteron group leading to the state at 1.4-MeV excitation in the reaction $Fe^{56}(p,d)Fe^{55}$. The solid curve is a distorted-wave Born-approximation calculation.

apparent from the (p,d) spectra that this approach is inadequate, and that residual interactions must be taken into account in some manner. For example, the appearance of two well-separated $l=1$ groups in the $Fe^{58}(p,d)$ spectrum suggests that the four neutrons above 28 cannot be regarded as filling a fourfold-degenerate $p_{3/2}$ shell.

The difference between the Co^{59} and the Fe^{58} spectra indicates that there is a strong interaction between the protons and neutrons; the simplest model predicts that these spectra would be alike. The spectra cannot be explained simply by considering the different possible couplings of the odd-proton spin with the spin of the neutron hole created in the pickup reaction; the Co^{59} spectrum is actually simpler than the Fe^{58} spectrum. In fact, the $Co^{59}(p,d)$ spectrum is almost what would be expected from the spherical potential shell model. It appears that the odd proton in Co^{59} has restored the $p_{3/2}$ degeneracy which was somehow removed for Fe^{58}.

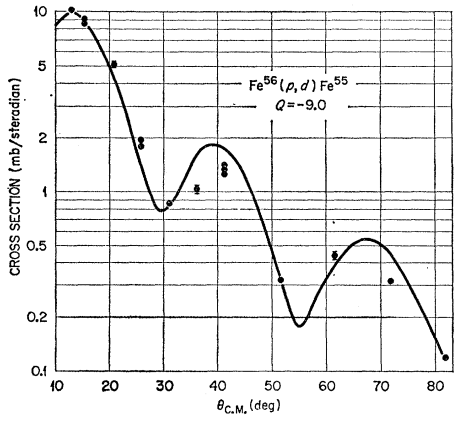

FIG. 9. Angular distribution of the deuteron group leading to the ground state in the reaction $Fe^{56}(p,d)Fe^{55}$. The solid curve is a distorted-wave Born-approximation calculation.

The data also seem to rule out the possibility of regarding the 28 neutrons in Fe^{54} as a closed-shell core which is undisturbed by the addition of 2, 3, or 4 neutrons to make Fe^{56}, Fe^{57}, or Fe^{58}. Attempts to analyze (d,p) and (d,t) reaction data in terms of a shell model modified by residual interactions involving only the particles outside the 28 shell have been made.[8] The $Fe^{56}(p,d)$ data, however, seem to indicate the existence of a strong interaction between the p-shell neutrons and the f-shell core. We regard the deuteron group from the $Fe^{54}(p,d)$ reaction at $Q=-11.2$ MeV as due to removal of an $f_{7/2}$ neutron. In the $Fe^{56}(p,d)$ reaction the group at $Q=-10.4$ MeV (corresponding to an excitation of 1.4 MeV in Fe^{55}) has the same angular distribution and nearly the same absolute cross section as the $Q=-11.2$ MeV group from Fe^{54}. The spin and parity of a level at 1.4 MeV in Fe^{55} are known to be $7/2-$, so that it seems reasonable that the deuteron group at $Q=-10.4$ MeV (which corresponds to that level) is associated with the pickup of an $f_{7/2}$ neutron. This indicates that the addition of two neutrons to Fe^{54} not only reduces the binding energy of the $f_{7/2}$ neutrons by 0.8 MeV but also affects the core in such a way that another f state can be created by removal of a neutron from Fe^{56} at $Q=-11.9$ MeV.

The state at $Q=-11.9$ MeV apparently involves core excitation. If an attempt is made to preserve the picture of Fe^{56} as an Fe^{54} core plus two neutrons, and to interpret the state reached by $Fe^{56}(p,d)Fe^{55}$ at $Q=-11.9$ MeV as a single particle state of an Fe^{54} core plus one neutron, the state must be considered as the $f_{5/2}$ single-particle state. This interpretation requires the assumption of a strong admixture of $(f_{5/2})^2$ in the ground state of Fe^{56}, since the reduced width for exciting the f state is larger than that for exciting the $p_{3/2}$ ground state of Fe^{55}. Schiffer *et al.*[9] assume an almost pure $(f_{5/2})^2$ ground state for Fe^{56} to account for the $Fe^{56}(d,p)$ cross section. If such as assignment for Fe^{56} is correct, then in the spirit of our treatment it should be possible to view the (p,d) reaction as a simple pickup from a partially filled $f_{5/2}$ shell with the Q value indicative to the $f_{5/2}$ single-particle binding energy plus pairing energy. This would place the $f_{5/2}$ level below the $f_{7/2}$ level, contrary to the well-established sign of the shell-model spin-orbit splitting. Even if the assumption is made that configuration mixing of $(p_{3/2})^2$ and $(f_{5/2})^2$ shifts the apparent positions of the bound states so that the Q values do not measure the single-particle binding energies in a simple way, the assumed interpretations of the levels in Fe^{55} still locate the single-particle bound states. The assumptions place the $f_{5/2}$ particle state at 2.9 MeV above the $p_{3/2}$ particle state and 1.5 MeV above the $f_{7/2}$ hole state. The assumed configuration mixing seems inconsistent with

[8] B. J. Raz, B. Zeidman, and J. L. Yntema, Phys. Rev. **120**, 1730 (1960).

[9] J. P. Schiffer, L. L. Lee, Jr., and B. Zeidman, Phys. Rev. **115**, 427 (1959).

TABLE II. Ratios of observed cross sections to cross sections calculated from distorted-wave Born-approximation theory.

Target nucleus	Q (MeV)	Δl	Final nucleus	Excitation energy (MeV)	Spectroscopic factor, S	Comment
Fe^{54}	−11.2	3	Fe^{53}	0	3.3±0.1	Probably single level
Fe^{56}	− 9.0	1	Fe^{55}	0	0.77±0.04	Two levels
Fe^{56}	− 9.4	1	Fe^{55}	0.4		
Fe^{56}	−10.4	3	Fe^{55}	1.4	2.7±0.2	Probably single level
Fe^{56}	−11.9	3	Fe^{55}	2.9	1.25±0.05	Probably single level
Fe^{57}	− 5.4	1	Fe^{56}	0	0.062±0.004	Single level
Fe^{57}	− 6.2	1	Fe^{56}	0.8	0.35±0.03	Single level
Fe^{57}	− 7.5	3	Fe^{56}	2.1	0.13±0.03	Single level
Fe^{57}	− 8.5	1	Fe^{56}	3.1	0.65±0.1	Not single level
Fe^{57}	− 9.7	3	Fe^{56}	4.3	3.2±0.6	Not single level
Fe^{58}	− 7.9	1	Fe^{57}	0	0.93±0.07	Not single level
Fe^{58}	− 9.0	1	Fe^{57}	1.1	0.53±0.04	Not single level
Fe^{58}	−10.0	3	Fe^{57}	2.1	3.6±0.4	Not single level
Co^{59}	− 8.0	1	Co^{58}	0	1.08±0.05	Not single level
Co^{59}	−10.8	3	Co^{58}	2.8	2.7±0.3	Not single level

this separation and with the large reduced width observed for this state. We feel that the picture of the Fe^{56} ground state as an Fe^{54} core plus two neutrons is inadequate, and that the picture of the f state at 2.9 MeV in Fe^{55} as the $f_{5/2}$ single-particle state is incorrect.

If the single-particle states from which the neutrons are removed by the reaction are assumed to be the bound states in a spheroidal potential as calculated by Nilsson,[10] a qualitatively correct pattern of levels is obtained for the (p,d) spectra. Since the $Fe^{54}(p,d)$ and the $Co^{59}(p,d)$ spectra are in agreement with the predictions of the spherical-potential shell model, these nuclei are assumed to be spherical. Fe^{56}, Fe^{57}, and Fe^{58} are assumed to be deformed to a prolate spheroidal shape.

Summation of the Nilsson single-particle energies to the appropriate neutron and proton numbers in fact indicates a favoring of a prolate shape for Fe^{56}, Fe^{57}, and Fe^{58} and a favoring of a spherical shape for Fe^{54} and Co^{59}. Table III shows the difference between the sum of single-particle energies for the spherical case and for the deformed case for several values of δ. The parameter δ is defined in reference 9. Identical binding energies are assumed for proton and neutron states, and the eigenvalues used in this summation are those given in Table I of reference 9; the energy scale is that suggested in the reference.

TABLE III. Change in the sum of single-particle binding energies caused by deformation of the potential. The deformation parameter used in this calculation are those of Table I, of reference 9.

	ΔE (Mev)				
Nucleus	$\delta=-0.2$	$\delta=-0.1$	$\delta=0.0$	$\delta=0.1$	$\delta=0.2$
Fe^{54}	4.88	0.70	0.0	0.11	5.60
Fe^{56}	2.92	−0.23	0.0	−1.36	4.96
Fe^{57}	3.14	−0.20	0.0	−1.22	5.21
Fe^{58}	3.37	−0.17	0.0	−1.09	5.45
Co^{59}	4.53	0.37	0.0	−0.01	6.66

Consider Fe^{58}, for example. In its ground state, if δ is approximately 0.15, all the Nilsson orbits through number 14 are filled with neutrons, as are orbits 17 and 20 (see Fig. 10). We associate the peak at $Q\sim-8$ MeV in the $Fe^{58}(p,d)Fe^{57}$ spectrum with those states in Fe^{57} generated by creating a single hole in orbit 20. Similarly, we associate the peak at $Q=-9$ MeV with a hole in orbit 17, and the peak at $Q\sim-10$ MeV with a hole in orbit 10. Since the pairing energy for the $\Omega=7/2$ orbit 10 is expected to be larger than that for the $\Omega=1/2$ orbit 17 and larger than the separation of the states, there is some ambiguity concerning the order of the states. The model is not expected to be valid in predicting the exact level positions in this situation. Comment on this point is made below.

Co^{59} is assumed to be spherical in its ground state with a neutron configuration of a filled $f_{7/2}$ shell and a

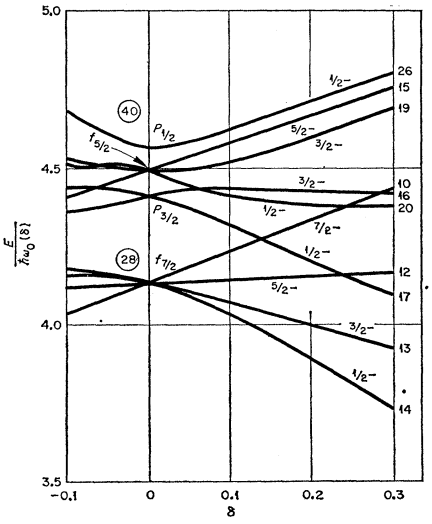

FIG. 10. Energies of the single-particle states in the $2p$ $1f$ shell region for a deformed nucleus.[10]

[10] S. G. Nilsson, Kgl. Danske Videnskab. Selskab, Mat.-fys. Medd. **29**, No. 16 (1955).

filled $p_{3/2}$ shell. The proton configuration is one hole in the $f_{7/2}$ shell. We associate the peak in the $Co^{59}(p,d)$ spectrum at $Q\sim-8$ MeV with the creation of one hole in the $p_{3/2}$ shell. The peak presumably includes the four possible spin states due to coupling the $p_{3/2}$ neutron hole with the $f_{7/2}$ proton hole in Co^{58}. The 2+ state is the ground state, and the 5+ state is at 25 keV.[11] We infer from the (p,d) spectrum that the other two states, 3+ and 4+, have excitations of a few hundred keV.

Pickup of an $f_{7/2}$ neutron from Co^{59} cannot be so simply pictured. Of the possible states which can be created by removal of an $f_{7/2}$ neutron, one is a 0+ state which is the Nilsson analog of the ground state of Fe^{58} in the approximation that the neutron and the proton binding forces are the same, i.e., this state has one proton and one neutron in orbit 10 ($\Omega=7/2$) with opposite signs of Ω. Since it is assumed that a prolate shape is energetically favored for the ground state of Fe^{58}, it must also be assumed that this is the case for this 0+ excited state of Co^{58}. Thus, the Q value for creation of this state by the $Co^{59}(p,d)$ reaction should be less negative than the value expected from the binding energy of an $f_{7/2}$ neutron in a spherical potential. The same argument applies to the 7+ state of Co^{58}, however, the other states corresponding to the removal of an $f_{7/2}$ neutron might be regarded as ordinary $f_{7/2}$ hole states.

We associate the complex peak at $Q=-10.9$ MeV in the $Co^{59}(p,d)$ spectrum with the 0+ and 7+ states and assert that the Q value is not a simple measure of the spherical potential binding energy.

A similar situation occurs in the $Fe^{56}(p,d)$ reaction. In this case removal of a neutron from Nilsson orbit 17 ($\Omega=1/2-$) has a restoring tendency and could result in a spherical nucleus with an odd neutron in the $p_{3/2}$ shell (the ground state of Fe^{55}). Removal of a neutron from orbit 10 ($\Omega=7/2-$) would, however, create a spin 7/2 state which maintains the prolate deformation of Fe^{56}. We interpret the peak in the $Fe^{56}(p,d)$ spectrum as corresponding to this 7/2− state. The energy corresponds to the excitation of a known 7/2 state at 1.4 MeV in Fe^{55}.

This approach suggests that the peak at $Q\sim-11.9$ MeV should be associated with a hole in Nilsson orbit ($\Omega=5/2-$), which would maintain the prolate shape.

The $Fe^{57}(p,d)$ spectrum is more complicated than the spectra from even-N targets. A possible interpretation is that the peaks at $Q=-5.4$, -6.2, and -7.4 MeV are associated with the removal of the odd neutron from orbit 20 ($\Omega=1/2-$). This is consistent with saying that the 2+ and 4+ levels in Fe^{56} at 0.8 and 2.0 MeV, respectively, are collective states built on the ground-state single-particle configuration of Fe^{56} and that the (p,d) reaction excites these collective states. We expect to find peaks analogous to those in $Fe^{56}(p,d)$ due to removal of a neutron from orbit 17 and due to removal of a neutron from orbit 10. We assign the broad and complex peaks around $Q\sim-8.5$ MeV and $Q\sim-9.7$ Mev to these pickups, and we assume that the complexity in these cases involves not only coupling with collective modes, but also interaction of the hole with the odd particle in orbit 20. This interpretation seems quite reasonable since the $Fe^{57}(p,d)$ spectrum, excluding the three states discussed above, looks very much like a smeared-out $Fe^{56}(p,d)$ spectrum with the general character of the angular distributions preserved.

Our use of the Nilsson model is in one respect essentially different from the approach of Lawson and Macfarlane[12] and Vervier and Bartholomew[13] in their application of the model to Fe^{57}. In those treatments the deformation is a parameter which is fixed for the given nucleus. Thus the model provides a Hamiltonian of which the eigenstates are interpreted as energy levels of that nucleus. Since we determine a deformation for each single-particle configuration we are not left with a fixed Hamiltonian for the nucleus. We do not seriously worry about this problem since we do not propose the Nilsson model as a complete theoretical treatment of the energy levels in the iron isotopes. Other difficulties with the treatment could, in fact, be pointed out. For example, the pairing energy is included as an independent effect in spite of the fact that the pairing energy is larger than the separation of the single-particle states.

The intention here is to point out the need to take residual interactions into account and to point out that the Nilsson model provides a means of doing this in a way which is useful for cataloging and "understanding" the features of the (p,d) spectra.

It is interesting to examine corroborative evidence for the assumption that several of the iron isotopes are deformed. Quadrupole moments would provide direct evidence, but unfortunately the ground-state spins of all the iron isotopes are zero or one-half so that quadrupole moments cannot be measured. Three measured

TABLE IV. Excitation energies of the first 2+ levels for even-even nuclei near iron.

Nucleus	Z	N	$E(2^+)$ (MeV)	Comment
Cr^{52}	24	28	1.45	Spherical
Cr^{54}	24	30	0.84	Deformed
Fe^{54}	26	28	1.41	Spherical
Fe^{56}	26	30	0.845	Deformed
Fe^{58}	26	32	0.805	Deformed
Ni^{58}	28	30	1.45	Spherical
Ni^{60}	28	32	1.33	Spherical

[11] *Nuclear Data Sheets* [National Research Council (National Academy of Sciences), Washington, D. C.].

[12] R. D. Lawson and M. H. Macfarlane, Nuclear Phys. **24**, 18 (1961).

[13] Vervier and G. A. Bartholomew, Proceedings of the International Conference on Nuclear Structure (University of Toronto Press, Toronto, 1960), p. 441.

quadrupole moments are, however, of interest—that of the 14-keV state in Fe^{57} and those of the ground states of Mn^{55} and Co^{59}. The Fe^{57} positive quadrupole moment of about 0.1 b[14] is consistent with the deformation expected from the (p,d) analysis. This moment of 0.1 b corresponds to $\delta \approx 0.1$.

The measured quadrupole moment of Co^{59} of 0.4 b[15] is not out of line with the expected quadrupole moment of an odd-proton spherical nucleus.[16] On the other hand the measured quadrupole moment of Mn^{55} is as large as that of Co^{59}, although the spherical shell model predicts that it should be only one third as large. A discussion of the large quadrupole moment of Mn^{55} and the unusual spin of 5/2 for the ground state of that nucleus is given in reference 16, and it is suggested that a deformation might be responsible for the unusual coupling and the large quadrupole moment.

Mn^{55} and Fe^{56} have the same number of neutrons. Summation of the Nilsson single-particle energies suggests prolate deformations for Mn^{55} as well as for Fe^{56}. Such a deformation explains both the ground-state spin and the quadrupole moment of Mn^{55}.

The assumptions about the deformations also correlate with the locations of the first 2+ excited states of the even-even nuclei. In the nuclei which are assumed to be spherical, this state, which probably is a vibrational state, is high; in the nuclei which are assumed to be deformed, this state is low. The locations of the 2+ excited states for the even iron and nickel isotopes are listed in Table IV. These states are strongly excited in inelastic proton scattering; analogous peaks appear in the inelastic proton spectra for some odd isotopes. The inelastic proton spectra for the targets used in this work are shown in Figs. 11–15. Note that the first inelastic peak for Co^{59} occurs at about 1.3-MeV excitation, which corresponds to a spherical rather than a deformed case. For Fe^{57} there is no apparently analogous level. This is consistent with the interpretation that Fe^{57} is deformed.

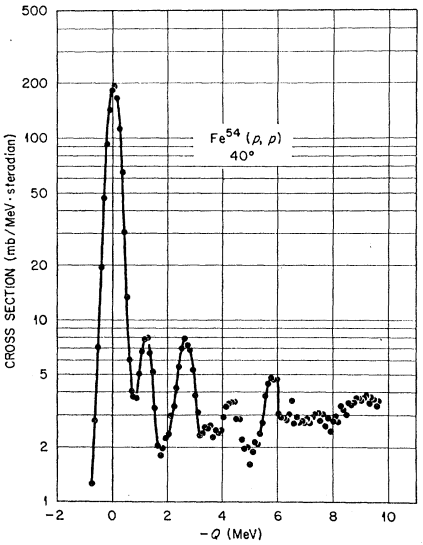

FIG. 11. Spectrum of scattered protons from bombardment of Fe^{54} with 22.3-MeV protons.

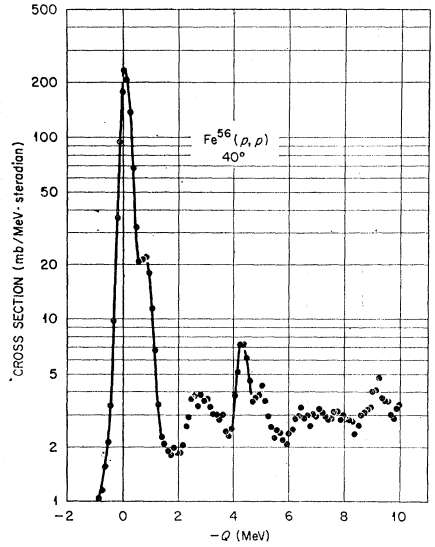

FIG. 12. Spectrum of scattered protons from bombardment of Fe^{56} with 22.3-MeV protons.

CONCLUSION

The (p,d) energy spectra from the iron isotopes and from cobalt show pronounced structure and only a

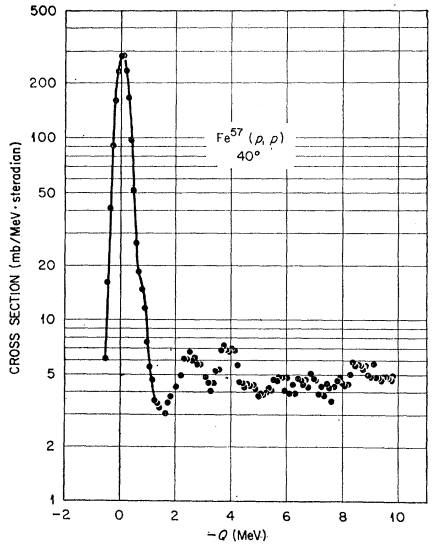

FIG. 13. Spectrum of scattered protons from bombardment of Fe^{57} with 22.3-MeV protons.

[14] A. Abragam and F. Boutron, Compt. rend. **252**, 2404 (1961).
[15] D. v. Ehrenstein, H. Kopfermann, and S. Penselin, Z. Physik **159**, 230 (1960).
[16] M. G. Mayer and J. H. D. Jensen, *Elementary Theory of Nuclear Shell Structure* (John Wiley & Sons, Inc., New York, 1955), p. 106 ff.

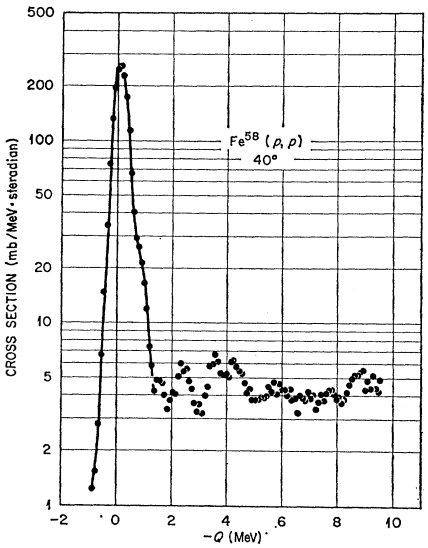

FIG. 14. Spectrum of scattered protons from bombardment of Fe^{58} with 22.3-MeV protons.

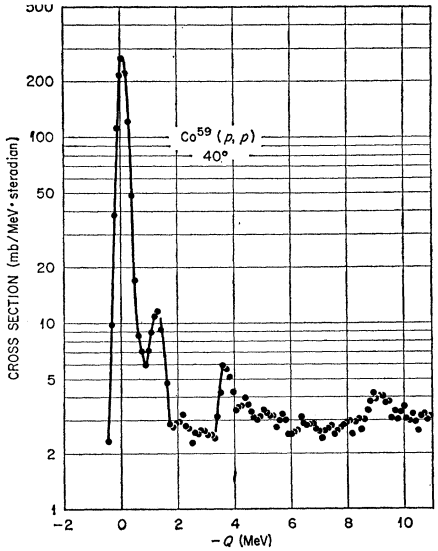

FIG. 15. Spectrum of scattered protons from bombardment of Co^{59} with 22.3-MeV protons.

few of the many known energy levels are excited with large cross sections. The corresponding deuteron groups have angular distributions expected for angular momentum changes of one and of three units. In this respect the data suggest the applicability of the *j-j* coupling shell model.

Some significant departures from the predictions of this model are noted. Nevertheless, it is felt that a model should not depart too radically from this one if it is to be successful. We invoke the Nilsson model as a slight departure from the simple *j-j* coupling shell model. Essentially the model generalizes the simpler model by removing the restriction that the harmonic oscillator part of the potential be spherically symmetric. This change alone provides a qualitatively correct energy-level scheme and correctly predicts that Fe^{54} and Co^{59} differ qualitatively from Fe^{56}, Fe^{57}, and Fe^{58}.

We have not made any explicit use of the collective implications of the model nor have we made a serious attempt to adjust the parameters of the model to fit the data precisely. We do not expect any detailed fitting of parameters to be significant since the model does not include pairing energy, and, as was noted above, the pairing interaction energy is larger than the separation of single-particle levels. A determination of the deformation made by fitting the binding energies of the neutrons as determined from the (p,d) experiment is very sensitive to the assumed pairing energy and we feel that parameter fitting is meaningful only with a model that includes the pairing energy.

The data provide information about which levels of one nucleus have maximum parentage overlap with the ground state of the next higher isotope. In a sense, the single-particle states are found, but the concept of single-particle states is not model independent and one must use caution in interpreting these as the single-particle states of the *j-j* coupling model, since considerable departures from that model were noted.

ACKNOWLEDGMENTS

We wish to express our thanks to the cyclotron groups at Argonne National Laboratory and at Los Alamos Scientific Laboratory for generous assistance in obtaining targets. We also owe thanks to Carl A. Levinson for the suggestion of the possible applicability of the Nilsson model to iron nuclei.

The assistance of many people within Oak Ridge National Laboratory made this work possible. We single out for special thanks G. R. Satchler and R. H. Bassel for performing distorted-wave pickup calculations, A. E. Pugh for data taking, E. L. Olson for assistance with the electronics, A. W. Riikola for supervising the operation of the cyclotron, and R. S. Livingston for providing support for the project. We also thank the Instrumentation and Controls Division for providing us with thin surface barrier counters.